Journal of Alloys and Compounds, 187 (1992) 145–156
JALCOM 294

The synthesis, structure and characterization of $SrMoO_{2.6}{}^{15}N_{0.4}$

Guo Liu
Institute for Materials Research, McMaster University, Hamilton, Ont., L8S 4 M1 (Canada)

Xinhua Zhao* and H. A. Eick†
Department of Chemistry and Center for Fundamental Materials Research, Michigan State University, East Lansing, MI 48824–1322 (USA)

(Received February 11, 1992; in final form March 6, 1992)

Abstract

The structure of the cubic perovskite-type oxide-nitride $SrMoO_{2.6}N_{0.4}$, synthesized from $SrMoO_4$ and NH_3(g) at 750 °C, has been determined by neutron diffraction. Structural and chemical analyses suggest that the average Mo oxidation number is +4.4; nitrogen and oxygen atoms are distributed statistically in the anion sites. Magnetic susceptibility and electrical conductivity measurements suggest metallic behavior for this oxide-nitride; IR data are also presented. So that ^{15}N-enriched specimens could be synthesized, relationships in the synthesis reaction between total system pressure, partial pressure of NH_3(g), reaction time and the nitrogen content of the product $SrMo(O,N)_3$ were determined. These results are presented and discussed.

1. Introduction

Some pseudoternary alkaline earth–transition metal oxide-nitride perovskite-type compounds appear to exhibit interesting magnetic and electrical properties. Perovskite-type $MTaO_2N$, where M≡Ca, Sr or Ba, and $BaNbO_2N$ were prepared by heating the following in NH_3(g) at 950–1000 °C: for M≡Ba, mixtures of $BaCO_3$ and M_2O_5 homogenized under alcohol, and for M≡Ca or Sr, the appropriate $A_2B_2O_7$ phase [1]. $Ba_{1-x}Sr_xTaO_2N$ was synthesized either from mixtures of the oxide-nitrides or from a mixture of the carbonates and Ta_2O_5 heated in NH_3(g) [2]. Although these compounds were highly colored, no paramagnetic phase could be detected in the product. Even though neutron diffraction showed that the structure of $SrTaO_2N$ was tetragonal, the nitrogen and oxygen atoms were distributed statistically [2]. The perovskite-type oxide-nitrides $LnWO_xN_{3-x}$ $(0.6<x<0.8)$ were prepared by heating $Ln_2W_2O_9$ in NH_3(g) at 700–900 °C [3]. The W atoms exhibited a mixed V/

*On leave from the Department of Chemistry, Beijing Normal University, Beijing 100875, China.

†Author to whom correspondence should be addressed.

0925-8388/92/$5.00

VI oxidation state and the phase showed semiconductivity over the temperature range 100–500 K with conductivity values of 10–15 Ω^{-1} cm^{-1} [3]. Thermal power measurements indicated negative charge carriers; magnetic properties were not reported. Oxide-nitrides of the type $LaVO_{3-x}N_x$ ($0<x<0.9$) were also prepared by heating the oxide $LaVO_4$ in NH_3(g) at 650–850 °C [4]. These compounds exhibited p-type semiconductivity; no semiconductor–metal transition was observed for any of the compositions examined.

The perovskite-type $Ln^{III}Ti^{IV}O_2N$ (Ln = La to Yb) and $Ln^{III}B^{V}ON_2$ (Ln = La to Dy; B = Ta, Nb) were also synthesized by reaction of ternary oxides with NH_3(g) at about 950 °C [5]. For the Ti-containing compounds the reactants were the oxides $Ln_2Ti_2O_7$; for the Nb and Ta compounds they were LnTa(Nb)O_4. The $LaTiO_2N$ compound could be indexed on cubic symmetry, but data on the Ln = Nd phase demonstrated that the true symmetry was that of the orthorhombic $GdFeO_3$-type structure. The compounds LaTa(Nb)ON_2 and $NdTaON_2$, although also apparently cubic, are in fact, like $SmTaON_2$, of the orthorhombic $GdFeO_3$-type structure. A pyrochlore-type oxide-nitride was reported for Ln = Dy, and the Ln = Eu system was unique with europium apparently reduced by NH_3(g) to the divalent state.

Related oxide-nitrides include the Scheelite-type $KOsO_3N$ [6] and $LnWO_3N$ (Ln = Nd, Sm, Gd, Dy) [7], $CsOsO_3N$ [8] which has a structure related closely to that of $BaSO_4$, and the K_2NiF_4-type A_2TaO_3N (A = Ca, Sr and Ba [9]). In most of these compounds the anions are distributed statistically.

Perovskite-type $SrMoO_3$ and $BaMoO_3$ exhibit metallic conductivity [10] and their magnetic susceptibilities are temperature independent over almost the entire range between liquid helium and room temperature [11]. We wondered if partial substitution of N^{3-} for O^{2-} in $MMoO_3$ (M = Sr and Ba) would yield compounds with molybdenum in a mixed oxidation state, thereby significantly altering the compound's magnetic and electrical properties. Preliminary studies [12] suggested this hypothesis to be true. Since we needed ^{15}N-enriched specimens to undertake an NMR investigation [13], we studied the relationships among the partial pressure of NH_3(g), reaction time, product nitrogen content and phase purity. We report here the structure, synthesis, and the magnetic and electrical properties of $SrMoO_{2.6}N_{0.4}$.

2. Experimental method

The reactants were MoO_3 (99.5%, reagent grade, Merck, Inc., Rathway, NJ); $Sr(NO_3)_2$ (ACS certified, Fisher Scientific, Fair Lawn, NJ); $^{15}NH_3$(g) (99.9 atom% ^{15}N, Isotec, Inc., Woburn, MA) and NH_3(g) (Matheson, E. Rutherford, NJ). Both NH_3 reactants were purified prior to use by condensation with liquid nitrogen and subsequent distillation. The phase purity of $SrMoO_4$ which had been synthesized from MoO_3 that was dissolved in $NH_3 \cdot H_2O$ and precipitated with $Sr(NO_3)_2$(aq) was confirmed by X-ray powder diffraction.

Synthesis was effected by two procedures. The first involved heating $SrMoO_4$(s) confined in Pt or Ag crucibles and supported in Al_2O_3 boats at

750 °C for 48 h in flowing NH_3 [12]. The second utilized a closed system of about 600 ml in which the gases were circulated by a Masterflex peristaltic pump; NaOH(s) served as desiccant. The $SrMoO_4$ specimen was confined in a small quartz container supported in an alumina boat. The pressure in the system was monitored with a Hg manometer and a cathetometer, both to follow the progress of the reaction and to protect the system against over-pressure. Experiments were begun only when the system vacuum varied by less than 5 Torr per 24 h. X-ray powder diffraction analysis was effected with monochromatized Cu $K\alpha_1$ ($\lambda = 1.54050$ Å) radiation with a Guinier camera of 114.59 mm diameter and NBS certified silicon ($a = 5.43082(3)$ Å) as described previously [14]. The programs TREOR [15], APPLEMAN [16] and POWD12 [17] were utilized for indexing interplanar d-spacings, for lattice parameter refinement and for X-ray powder intensity calculations respectively. Nitrogen analyses were performed by Galbraith Laboratories, Inc., Knoxville, TN.

$SrMo(O,^{15}N)_3$ was also synthesized by reaction between $SrMoO_4$(s) and $^{15}NH_3$(g) at 750 °C. A room temperature $^{15}NH_3$(g) partial pressure of about 200 Torr prevented the system pressure at this temperature from exceeding atmospheric pressure and causing a concomitant loss of $^{15}NH_3$(g). As is described below, the reaction was forced to completion, *i.e.* until $SrMoO_4$(s) was no longer observed by X-ray powder diffraction, by periodically replacing the mixed gaseous reaction product. Specimen mass loss was monitored. Synthesis relationships, *i.e.* the total system pressure *vs.* reaction time and product weight loss *vs.* reaction time and partial pressure of NH_3(g) were determined with $SrMoO_4$ and normal NH_3 as reactants. The sample for neutron diffraction was prepared under comparable conditions with normal NH_3(g).

Room temperature neutron powder diffraction data were obtained at the McMaster nuclear reactor. A $SrMo(O,N)_3$ powder specimen weighing about 5 g was loaded into a thin-walled vanadium can and placed in the aluminum sample chamber which was evacuated. Data were collected at a temperature of 23(2) °C using a position-sensitive detector and 1.3913 Å neutrons as described previously [18]. Refinement was effected on a VAX computer with a modified version [18] of the Rietveld profile refinement program [19]. The R-factors reported are defined in ref. 18. The scattering lengths [20] used (units 10^{-12} cm) were: Sr, 0.702; Mo, 0.695; O, 0.5805; N, 0.930.

D.c. electrical measurements were effected by the standard four-probe method between 5 and 290 K. The powdered specimen was pressed into a pellet 6.3 mm in diameter to which copper wires were attached with silver paste. A.c. electrical measurements were also made by the four-probe method in the temperature range 85–295 K on a Hewlett–Packard 4192A LF impedance analyzer. The pressed polycrystalline $SrMoO_{2.6}N_{0.4}$ specimen had a diameter of 2.38 mm and a uniform thickness of 1.01 mm. Pressure-sensitive contacts were employed; the applied voltage was 1.00 V at 1 kHz.

Room temperature IR spectra for $SrMoO_{2.6}N_{0.4}$ specimens were obtained from 150 to 4000 cm^{-1} with a model 740 NICOLET FTIR spectrometer equipped with a SPECTRA TECH IR-Plan infrared microscope accessory for

the mid-IR range. Specimens with masses of about 0.1 g were prepared from finely ground powders pressed into pellets (at 25000 lbf in^{-2}) with KBr for mid-range data and with CsI for far-IR-range data. The KBr:$SrMoO_{2.6}N_{0.4}$ mass ratios were about 100:1; those of CsI:$SrMoO_{2.6}N_{0.4}$ were varied from 100:1 to 500:1.

Magnetic data were collected with Quantum Design SQUID magnetometers at various field strengths. Particular care was taken to remove O_2 from the systems. A diamagnetic correction was applied to derive the magnetic susceptibility. One data set in which each point represents the average of three scans was extrapolated to zero reciprocal field to eliminate ferromagnetic impurity contributions. Because of our concern that absorbed O_2 might be causing the transition observed around 50 K, the second data set was collected at McMaster University on a better-characterized specimen.

3. Results and discussion

3.1. $SrMoO_{2.6}N_{0.4}$ and its structure

Ground pulverized $SrMo(O,N)_3$ was colored dark blue to deep purple or violet in contrast with the deep red of $SrMoO_3$, and was not obviously either moisture- or air-sensitive. However, upon extended exposure to the laboratory atmosphere, the specimens oxidized slowly to $SrMoO_4$. The observed N content of specimens synthesized by the second procedure, 2.19%, suggests the formula $SrMoO_{2.64}N_{0.36}$. The composition determined from the neutron diffraction refinement ($SrMoO_{2.6}N_{0.4}$) is consistent with this formula. Thus, if we assume the oxidation state of nitrogen to be -3, the average molybdenum oxidation number is $+4.4$.

The X-ray powder diffraction pattern is essentially indistinguishable from that of $SrMoO_3$; both compounds are of the perovskite type (space group: *Pm3m*) with $a=3.9736(5)$ Å for $SrMoO_{2.64}N_{0.36}$ and 3.974 Å reported for $SrMoO_3$ [21]. (We obtained $a=3.9651(5)$ Å for $SrMoO_3$(s)). The lattice parameter $a=3.9765(3)$ Å was found for specimens prepared by the first procedure; [N]=3.09(3)%; formula $SrMoO_{2.5}N_{0.5}$ [12]. However, this apparently more precise parameter may be less accurate than the error suggests since it was derived from specimens with very small particle sizes and consequently broad diffraction reflections.) Because of the nearly identical X-ray scattering factors for nitrogen and oxygen, there is no obvious difference between the two X-ray diffraction patterns. Therefore, since oxygen and nitrogen have significantly different neutron scattering lengths, neutron diffraction is the method of choice for a structural study.

3.2. Structure refinement

Refinement was begun with the composition and parameters of $SrMoO_3$. Oxygen was then partially replaced by nitrogen with the constraints of an identical temperature factor for the anions and a total anion site occupancy of unity. Refinement converged upon introduction of nitrogen with the best

fit achieved at the composition $SrMoO_{2.6}N_{0.4}$. The R values before and after nitrogen substitution are compared in Table 1 and the refinement results for the $SrMoO_3$ and $SrMoO_{2.6}N_{0.4}$ compositions are compared in Table 2. The observed, calculated and difference profiles are plotted in Fig. 1; peak positions are marked below the difference profile.

The structural results confirm the cubic perovskite-type structure for $SrMoO_{2.6}N_{0.4}$. The refined lattice parameter a (neutron) = 3.9695(2) Å is

TABLE 1

Comparison of R values (%) for $SrMo(O,N)_3$ before and after nitrogen substitution

Composition	R_{exp}	R_n(nuclear)	R_p	R_{wp}
$SrMoO_3$	3.39	5.81	6.62	8.65
$SrMoO_{2.6}N_{0.4}$	3.39	5.01	6.23	8.27

TABLE 2

Comparison of the atomic thermal parameters derived from neutron diffraction for $SrMo(O,N)_3$ before ($SrMoO_3$) and after ($SrMoO_{2.6}N_{0.4}$) nitrogen substitution

Atom	Site	x	y	z	B (Å^2)	
					$SrMoO_3$	$SrMoO_{2.6}N_{0.4}$
Sr	1(b)	0.5	0.5	0.5	0.81(4)	0.59(8)
Mo	1(a)	0	0	0	0.54(5)	0.33(8)
O	3(d)	0.5	0	0	0.36(3)	0.55(6)
N	3(d)	0.5	0	0	–	0.55(6)

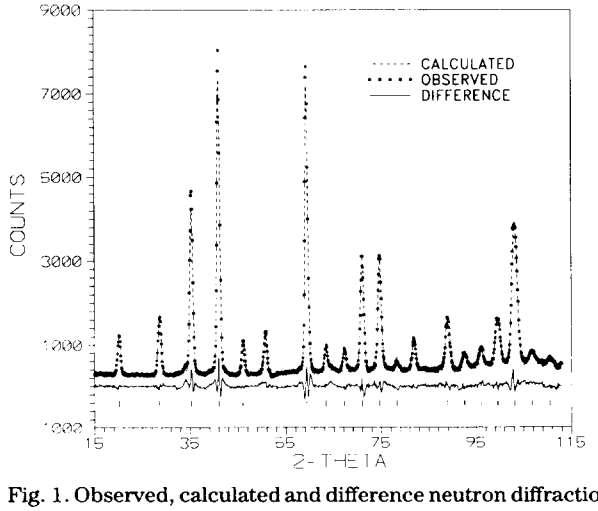

Fig. 1. Observed, calculated and difference neutron diffraction pattern for $SrMoO_{2.6}N_{0.4}$. Reflection positions are marked beneath the difference plot.

slightly shorter than the Guinier-determined value $a = 3.9736(5)$ Å, but is probably less accurate since the Guinier data were corrected with an internal silicon standard. Interatomic distances calculated with the neutron-refined lattice parameters are: 6 Mo–(O,N) at 1.9848(1) Å and 12 Sr–(O,N) at 2.8069(2) Å. The absence of superlattice reflections in the neutron diffraction pattern is consistent with a random anion distribution. The thermal parameter observed for the anions, 0.55(6) Å^2, compares favorably with those observed for other perovskite-type compounds: 0.7(2) and 0.5(2) Å^2 for $SrTaO_2N$ [2], 0.44(8) and 0.38(5) Å^2 for $LaWO_{0.6}N_{2.4}$ [21], and 0.69(2) and 0.55(2) Å^2 for $BaNbO_2N$ and $BaTaO_2N$ respectively [1].

3.3. Conductivity and magnetic data

The d.c. and a.c. electrical conductivity data are plotted in Fig. 2. In both cases the conductivity decreases slightly with decreasing temperature. Although this behavior is typical for semiconductors, the small change in magnitude over the entire temperature range and the high conductivity observed at 5 K do not support a semiconductor model. We believe the measured values are dominated by grain-boundary resistances. Since the samples tend to lose nitrogen upon sintering at high temperatures, we have not been able to measure true bulk conductivities. Nevertheless, the relatively low resistivities observed suggest that $SrMoO_{2.6}N_{0.4}$ is metallic. Evidence for metallic behavior is also given by the NMR experiments [13]. Attempts to collect MAS NMR data were unsuccessful because the conductivity of the specimens prevented them from spinning in the spectrometer.

It is noteworthy that the d.c. resistivities are about two orders of magnitude higher than the a.c. values, probably because d.c. measurements are more sensitive to grain-boundary resistances. Typical a.c. resistivity values for

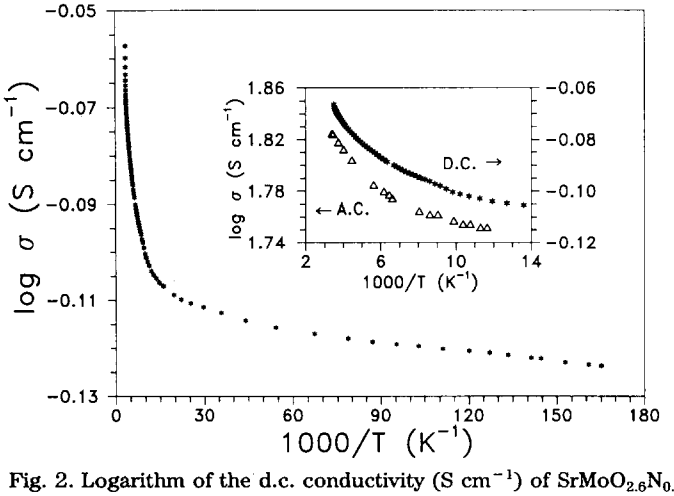

Fig. 2. Logarithm of the d.c. conductivity (S cm^{-1}) of $SrMoO_{2.6}N_{0.4}$ *vs.* reciprocal temperature. Insert: comparison of a.c. (Δ, left ordinate) and d.c. (*, right ordinate) against reciprocal temperature.

$SrMoO_{2.6}N_{0.4}$ are 1.50×10^{-2} Ω cm at 294 K and 1.77×10^{-2} Ω cm at 86 K. The oxide analogue, $SrMoO_3$, whose structure is nearly identical with that of $SrMoO_{2.6}N_{0.4}$ as described above, is also metallic with a room temperature resistivity of 7.82×10^{-5} Ω cm for powder specimens sintered at 1200–1500 °C [10]. Thus partial substitution of nitrogen for oxygen in perovskite-type $SrMoO_3$ does not change its electrical properties dramatically. Similar behavior was also observed for the perovskite-type semiconductor $LaVO_3$ [4]; $LaVO_{3-x}N_x$ ($0<x<0.9$) compounds remained semiconducting upon partial substitution of nitrogen for oxygen.

Magnetic data for $SrMoO_{2.6}N_{0.4}$ are plotted as $1/\chi$ *vs.* temperature in Fig. 3. Data points for the curve to the left were taken at an applied magnetic field of 2000 gauss; those to the right were extrapolated to zero reciprocal magnetic field to eliminate contributions from ferromagnetic impurities. Diamagnetic corrections are made for both curves. The extrapolated values are about two to three times smaller than those at 2000 gauss and should represent the true magnetic susceptibilities of $SrMoO_{2.6}N_{0.4}$.

The feeble paramagnetic susceptibility appears to be independent of the temperature down to 90 K. This result also supports the metallic model for the oxide-nitride. The extrapolated room temperature susceptibility for $SrMoO_{2.6}N_{0.4}$, 1.23×10^{-4} emu mol^{-1}, is slightly smaller than that for $SrMoO_3$, 2.01×10^{-4} emu mol^{-1} [11]. Although the susceptibility of $SrMoO_3$ remains constant to within 3% almost down to liquid helium temperatures [11], interesting features—a susceptibility maximum around 50 K—are observed for the oxide-nitride in the low temperature range. This maximum was initially suspected to result from liquified O_2 (m.p. 54.35 K; b.p. 90.18 K [22]) which

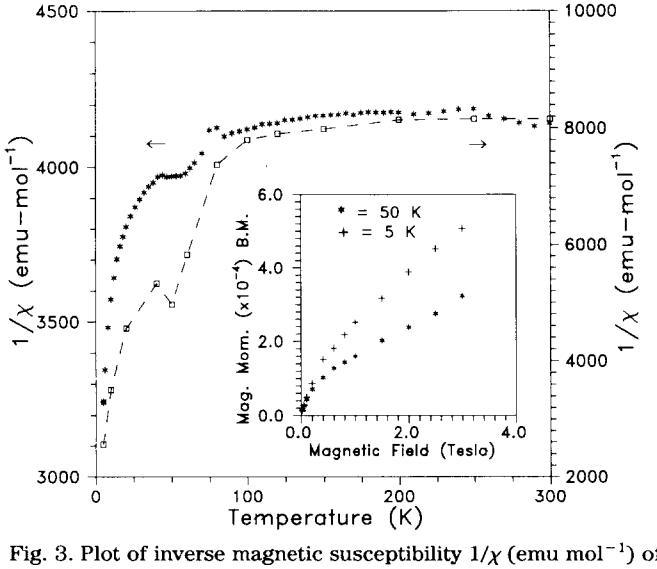

Fig. 3. Plot of inverse magnetic susceptibility $1/\chi$ (emu mol^{-1}) of $SrMoO_{2.6}N_{0.4}$ *vs.* temperature; sample a: □, extrapolated to infinite magnetic field; sample b: *, $2/\chi$, not extrapolated to infinite magnetic field. Insert: magnetic moment *vs.* magnetic field.

is paramagnetic and could contribute to the susceptibility maximum if trapped in the SQUID system, liquified and then frozen around the sample upon further cooling. However, the peak remained upon repeated experimentation when the specimen chamber was purged carefully prior to taking measurements. We believe it represents an antiferromagnetic transition. The rapid increase in magnetic susceptibility below 50 K is probably indicative of contamination by trace amounts of paramagnetic impurities. The magnetic moment *vs.* field curves inserted in Fig. 3 suggest the presence of ferromagnetic components.

3.4. IR data

The IR spectrum is presented in Fig. 4. It is relatively nondescript; a broad absorption band whose intensity decreases slowly from high to low wavenumbers spans the measurement ranges. An absorption peak is superimposed on this band at 870 cm^{-1}. Other weak absorptions at 2854 cm^{-1} and 2924 cm^{-1} result from interaction with the laboratory atmosphere. No absorption was found in the far IR range even though the sample was diluted in a stepwise fashion.

3.5. Synthesis procedure

One can imagine the synthesis reaction proceeding in two steps. The $SrMoO_4$(s) could react initially with NH_3(g) to yield either $SrMoO_3$(s) or $SrMoO_{3-x}N_x$(s), with $x<0.4$, and this product could in turn react further with NH_3(g) to produce a more nitrogen-rich product. The synthesis reaction would then be represented by eqns. (1) and (2), with eqn. (1) representing the reductive synthesis reaction and eqn. (2) the subsequent reaction with NH_3(g):

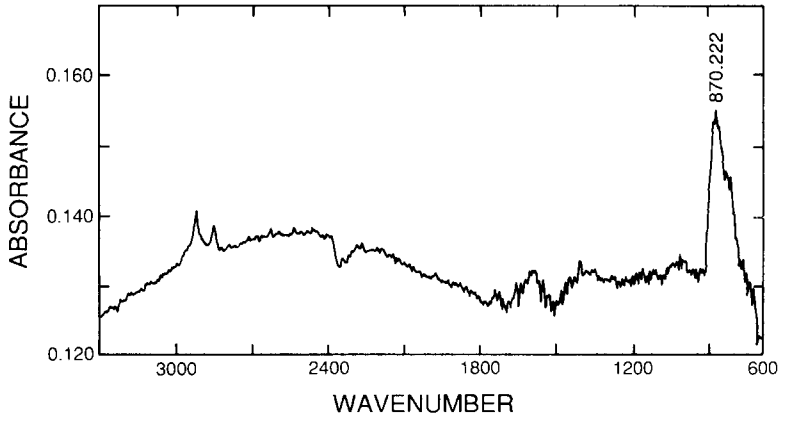

Fig. 4. IR absorption spectrum of $SrMoO_{2.6}N_{0.4}$ obtained by the CsI (KBr) pellet procedure.

$$SrMoO_4(s) + \frac{2+2x}{3} NH_3(g) \longrightarrow$$

$$SrMoO_{3-x}N_x(s) + (1+x)H_2O(g) + \frac{2-x}{6} N_2(g) \quad (1)$$

$$SrMoO_{3-x}N_x(s) + y\ NH_3(g) \longrightarrow$$

$$SrMoO_{3-x-y}N_{x+y}(s) + yH_2O(g) + \frac{y}{2} H_2(g) \quad (2)$$

Although the two-step process cannot be ruled out since X-ray powder diffraction data do not permit us to distinguish between $SrMoO_3(s)$ and $SrMoO_{2.6}N_{0.4}(s)$, we believe that eqn. (3), in which the $SrMoO_4(s)$ reacts directly with $NH_3(g)$ to produce $SrMoO_{2.6}N_{0.4}(s)$, is more consistent with the observations for two reasons.

$$SrMoO_4(s) + 0.934\ NH_3(g) \longrightarrow$$

$$SrMoO_{2.6}N_{0.4}(s) + 1.40\ H_2O(g) + 0.267\ N_2(g) \quad (3)$$

Firstly, the data presented in Table 3 indicate that $SrMoO_4(s)$ and the oxide-nitride phase are present in the reaction mixture with the quantity of the former decreasing as the reaction progresses. X-ray powder diffraction analyses of the product conducted as the reaction proceeded did not indicate the presence of any other phase (see Table 3). Secondly, in eqn. (1) $NH_3(g)$ acts as a reducing agent, whereas in eqn. (2) it must act as an oxidizing agent. Since both reactions occur simultaneously, such behavior is unlikely.

However, $NH_3(g)$ can also reduce $SrMoO_4(s)$ directly to $SrMoO_3(s)$ as indicated in eqn. (4):

$$3\ SrMoO_4(s) + 2\ NH_3(g) \longrightarrow 3\ SrMoO_3(s) + 3\ H_2O(g) + N_2(g) \quad (4)$$

TABLE 3

Relationships among mass loss, heating times and phases observed during synthesis of $SrMoO_{2.6}N_{0.4}$

No.[a] (i)	t (h)	$t_i - t_{(i-1)}$ (h)	Yield (%)	[N] (%)	M.L. (%)	Phase(s) observed
1	1	1	11	–	0.77	$SrMoO_4$
2	4	3	31	–	2.6	$SrMoO_4$
3	7	3	34	0.56	4.04	$SrMoO_4$, $SrMoO_{2.6}N_{0.4}$
4	12	5	67	1.2	5.88	$SrMoO_4$, $SrMoO_{2.6}N_{0.4}$
5	17	5	147	1.4	7.20	$SrMoO_4$, more $SrMoO_{2.6}N_{0.4}$
6	22	5	–	1.3	7.88	$SrMoO_4$, mostly $SrMoO_{2.6}N_{0.4}$

[a] i: interval number; t: total reaction time; yield: the ratio of mass loss observed to mass loss theoretical (M.L.(%) (obs)/M.L.(%) (th)) between intervals; [N] (%): nitrogen content in product as determined by Galbraith Laboratories, Inc.; M.L. (%): per cent mass loss observed. (Theoretical M.L. for $SrMoO_{2.6}N_{0.4}$ is 6.78%.)

The compound $BaMoO_4(s)$ reacts with $NH_3(g)$ to yield an oxide-nitride with a structure different from that of $BaMoO_3(s)$ [12]. In this reaction the oxide-nitride is usually contaminated with $BaMoO_3(s)$ which forms via reaction (4). Once formed, $BaMoO_3(s)$ cannot be converted to oxide-nitride. On the basis of these observations, we believe that $SrMoO_4(s)$ reacts directly with $NH_3(g)$ to yield the indicated oxide-nitride and also suspect that different preparations contain small but differing amounts of $SrMoO_3(s)$.

The reaction trend is apparent in Fig. 5. In curve (a) the total system pressure is plotted against time. The total pressure increases rapidly for the first 6 h of the reaction and more slowly thereafter. The slight increase that occurs during hours 12–22 suggests both that a pseudo-equilibrium condition is reached and that the partial pressure of $NH_3(g)$ is important in determining the progress of the reaction. Consequently, reaction times were limited to 12 h. After each 12 h period the gaseous mixture produced in the closed system was removed, the system recharged with ammonia, and the reaction restarted.

Thermal decomposition of $NH_3(g)$ into $H_2(g)$ and $N_2(g)$ occurs during the reaction; at the end of the reaction more non-condensable gases, presumed to be N_2 and H_2, were always present than could be accounted for on the basis of eqn. (3). Thus some of the pressure rise indicated in Fig. 5 results from this decomposition.

The experimental data substantiate the supposition that the procedure of dividing the reaction into several intervals by changing gases did indeed increase the yield. The mass loss data in Fig. 5, curve (b), where each point

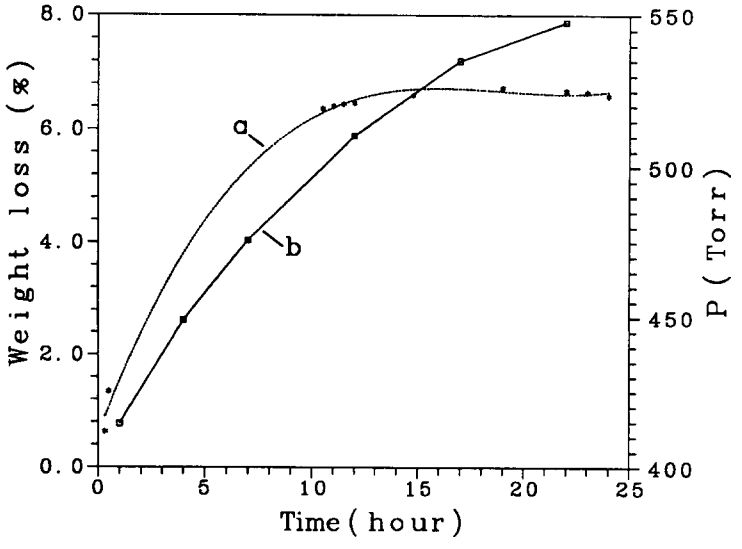

Fig. 5. Reaction of $SrMoO_4(s)$ with $NH_3(g)$. (a) Right ordinate: total system pressure *vs.* reaction time. The data points fit a third-order polynominal. (b) Left ordinate: mass loss *vs.* reaction time. Each point represents a recharging of the system with $NH_3(g)$.

represents a recharging of the system with $NH_3(g)$, show that the reaction can be forced to completion. The yield ((mass loss)$_{obs.}$/(mass loss)$_{calc.}$) increased as expected (see Table 3) with increasing time. However, the final mass loss observed (7.88%) was larger than the 6.78% expected for $SrMoO_{2.6}N_{0.4}$, probably because some MoO_3 was swept by transport from the reaction container during the extended heating.

The data show that the quantity of $SrMoO_{2.6}N_{0.4}$ in the product increased each time the system was recharged with $NH_3(g)$. The reason for this increase is clear. According to Le Chatelier's principle, the high partial pressure of $NH_3(g)$ should force the reaction, as illustrated in eqn. (3), to the right. Limiting the reaction time and recharging the system, in addition to maximizing the $SrMoO_{2.6}N_{0.4}$ yield, had the added benefit of minimizing the effect of minute quantities of air that might leak into the system.

Equation (2), if reaction proceeded by that route, would suggest that the nitrogen content could be increased further by increasing the partial pressure of $NH_3(g)$ above atmospheric pressure. Although extended heating in an $NH_3(g)$ atmosphere did not appear to increase the N content of the product, nitrogen analysis inaccuracies preclude our using these data to help establish the reaction pathway. The design of our synthesis system prevented our using a $NH_3(g)$ pressure in excess of one atmosphere.

Acknowledgments

We thank Professor John E. Greedan for the neutron diffractometer and SQUID time and for helpful discussions and Dr. Ruihe Huang for help in using the microscope to obtain the mid-range IR spectrum.

References

1 R. Marchand, F. Pors and Y. Laurent, *Rev. Int. Hautes Temp. Refract.*, *23* (1986) 11.
2 F. Pors, P. Bacher, R. Marchand, Y. Laurent and G. Roult, *Rev. Int. Hautes Temp. Refract.*, *24* (1987–1988) 239.
3 P. Antoine, R. Marchand, Y. Laurent, C. Michel and B. Raveau, *Mater. Res. Bull.*, *23* (1988) 953.
4 P. Antoine, R. Assabaa, P. L'Haridon, R. Marchand, Y. Laurent, C. Michel and B. Raveau, *Mater. Sci. Eng. B*, *5* (1989) 43.
5 R. Marchand, F. Pors and Y. Laurent, *Ann. Chim. (Paris)*, *16* (1991) 553.
6 Y. Laurent, R. Pastuszak, P. L'Haridon and R. Marchand, *Acta Crystallogr., Sect. B*, *38* (1982) 914.
7 P. Antoine, R. Marchand and Y. Laurent, *Rev. Int. Hautes Temp. Refract.*, *24* (1987) 43.
8 R. Pastuszak, P. L'Haridon, R. Marchand and Y. Laurent, *Acta Crystallogr., Sect. B*, *38* (1982) 1427.
9 F. Pors, R. Marchand and Y. Laurent, *Ann. Chim. (Paris)*, *16* (1991) 547.
10 L. H. Brixner, *J. Inorg. Nucl. Chem.*, *14* (1960) 225.
11 G. H. Bouchard, Jr., and M. J. Sienko, *Inorg. Chem.*, *7* (1968) 441.
12 Guo Liu, *Ph.D. Dissertation*, Michigan State University, E. Lansing, MI 48824–1322, 1990.
13 X. Zhao and H. A. Eick, to be published.

14 G. Liu and H. A. Eick, *J. Less-Common Met., 156* (1989) 237.
15 P. E. Werner, L. Eriksson and M. Westdahl, *J. Appl. Crystallogr., 18* (1985) 367.
16 D. E. Appleman, D. S. Handwerker and H. T. Evans, *Program X-Ray*, Geological Survey, US Department of the Interior, Washington, DC, 1966.
17 D. K. Smith, M. C. Nichols and M. E. Zolensky, *A FORTRAN IV Program for Calculating Powder Diffraction Patterns: Version 10*, Pennsylvania State University, University Park, 1983.
18 J. E. Greedan, A. H. O'Reilly and C. V. Stager, *Phys. Rev. B, 35* (1987) 8770.
19 H. M. Rietveld, *J. Appl. Crystallogr., 2* (1969) 65.
20 *File No. 24–1224, Powder Diffraction File, JCPDS*, 1983 (International Centre for Diffraction Data, 1601 Park Lake, Swarthmore, PA 19801).
21 P. Bacher, P. Antoine, R. Marchand, P. L'Haridon, Y. Laurent and G. Roult, *J. Solid State Chem., 77* (1988) 67.
22 N. N. Greenwood and A. Earnshaw, *Chemistry of the Elements*, 1st edn., Pergamon, 1984, reprinted with corrections, 1985, p. 706.